Selection rule for the optical absorption of graphene nanoribbons

Han Hsu and L. E. Reichl
Center for Complex Quantum Systems and Department of Physics, The University of Texas at Austin, Austin, Texas 78712, USA
(Received 7 March 2007; published 19 July 2007)

We demonstrate that the optical absorption of zigzag-edge graphene nanoribbons is qualitatively different from that of armchair nanotubes. Unlike the selection rule for nanotubes, when the incident beam is polarized along the longitudinal direction, the interband transitions at direct gaps are forbidden for graphene nanoribbons. This selection rule is due to the finite width of graphene nanoribbons. We also demonstrate that the edge states of graphene nanoribbons play an important role in the optical absorption. They are involved in many of the absorption peaks within optical range ($\hbar\omega < 0.12$ a.u.) and have no contribution to the absorption peaks beyond optical range.

DOI: 10.1103/PhysRevB.76.045418 PACS number(s): 78.40.Ri, 78.67.−n, 73.22.−f

I. INTRODUCTION

Carbon-based nanoscale low-dimensional materials, such as carbon nanotubes, single- or few-layer graphene, and graphene nanoribbons (finite-width strips made of graphene), have attracted much attention because of their properties and their potential in future application.[1–25] Recently, the study for graphene nanoribbons (GNRs) is a rapidly growing field.[3–15] The quasi-one-dimensional atomic structure of GNRs is similar to that of single-walled carbon nanotubes (SWNTs), but the electronic structures[3–9] and transport properties[10–15] of GNRs can be very different from that of SWNTs. As to optical properties, only a few graphene-based systems, such as few-layer graphene[16] and triangular graphene fragments,[17] have been studied, while SWNTs have been intensively studied in the past decade.[18–23]

In this paper, we study the optical response of GNRs in the perturbative regime, and we demonstrate that the optical absorption of GNRs is qualitatively different from that of SWNTs. For SWNTs, when the polarization of the incident beam is longitudinal, namely, parallel to the nanotube axis (x direction), the optical absorption peaks are mainly caused by the interband transitions at direct gaps, as explicitly discussed in Sec. III and some of the references.[20,21] Such a selection rule, however, does not apply to GNR. In the case of GNR, due to its finite width, the eigenstates are either symmetric or antisymmetric along the transverse direction (y direction), and the transitions at direct gaps are thus forbidden.

Another important feature of GNR is the existence of edge states, which do not occur in SWNTs and infinite graphene sheets. Edge states are electronic states that localize at (and extend along) the edge and decay exponentially into the center of GNR. The properties of edge states have been widely discussed in many theoretical works.[3–15] As shall be discussed later, edge states play an important role in optical absorption. They are involved in many of the absorption peaks in the optical range ($\hbar\omega < 0.12$ a.u.). Beyond optical range, they have no contribution to absorption peaks.

The atomic structure of GNR merits a brief review before we proceed to any further discussion. While SWNTs are generally categorized by the arrangement of carbon atoms along the cross section of the tube,[1,2] GNRs are categorized by the arrangement of carbon atoms on the side edges.[3] Two main types of GNR are zigzag-edge GNR (ZGNR) and armchair-edge GNR. Both types of GNRs can be further specified by their width, in other words, by the number of longitudinal atomic lines. For example, ZGNR with 12 zigzag lines is referred to as 12-ZGNR.[7,15] By comparing 12-ZGNR and (6, 6) SWNT, we will notice that for these two quasi-one-dimensional objects, the number of carbon atoms per unit strip is the same (24 atoms). If we roll up a 12-ZGNR and allow covalent bonds to connect the carbon atoms on opposite edges, a (6, 6) SWNT can be constructed.

Two cases will be considered in this paper: The case for (6, 6) SWNT and 12-ZGNR and the case for (10, 10) SWNT and 20-ZNGR. The relevant theoretical tools will be reviewed in Sec. II, and the results of calculations will be discussed in Sec. III. In Sec. IV, concluding remarks will be given.

II. THEORETICAL FORMULATION

It is well known that the electronic and optical properties of nanotubes and graphene are mainly determined by the π electrons of carbon atoms.[1,2] To model those π electrons, the tight-binding (TB) approximation has been widely used. The TB Hamiltonian H is written as

$$H = \gamma \sum_{\langle i,j \rangle} (|i\rangle\langle j| + |j\rangle\langle i|), \tag{1}$$

where $|i\rangle$ is the π state at site i, $\langle i,j\rangle$ represents pairs of nearest neighbor sites i and j, and $\gamma = -0.1115$ a.u. is the transfer integral. With this Hamiltonian, the band structure $E_{n,k}$ can be calculated, and the spatial symmetry of the eigenstates $|n,k\rangle$ can be determined by inspecting the eigenvectors, where n and k represent the nth energy level for a particular Bloch wave vector k.

In this paper, we compare the effect of external laser fields polarized longitudinal (referred to as x direction later) to SWNTs and GNRs. To study the response of SWNTs and GNRs to such fields, two quantities are useful: The joint density of states $D_j(\omega)$ and conductance $\sigma(\omega) = \sigma_1(\omega) + i\sigma_2(\omega)$. The joint density of states (JDOS) can be determined from the band structure using the formula

$$D_j(\omega) = \frac{2}{L} \sum_{n,n',k} [f(E_{n,k}) - f(E_{n',k})] \delta(E_{n',k} - E_{n,k} - \hbar\omega), \tag{2}$$

and the real part of conductance, $\sigma_1(\omega)$, which is directly related to the absorption of incident energy, can be calculated using perturbation theory[26] for the weak fields

$$\sigma_1(\omega) = \frac{2\pi e^2}{m_e^2 \omega L} \sum_{n,n',k} [f(E_{n,k}) - f(E_{n',k})] |\langle n,k|P_x|n',k\rangle|^2 \times \delta(E_{n',k} - E_{n,k} - \hbar\omega), \tag{3}$$

where L is the length of the nanoribbon (or nanotube), $f(E_{n,k})$ is the Fermi-Dirac distribution function, P_x is the x component of the momentum operator, and the factor of 2 is for spin degeneracy. Here, we assume $f(E_{n,k})=1$ for $E_{n,k}<E_F$ and $f(E_{n,k})=0$ for $E_{n,k}>E_F$. Since the on-site energy for the π electrons is chosen to be zero, the Fermi level E_F is zero for both ZGNR and SWNT.

In the presence of an incident laser beam with photon energy $\hbar\omega$, a peak in $\sigma_1(\omega)$ indicates an absorption peak for the photons with energy $\hbar\omega$, and vanishing $\sigma_1(\omega)$ indicates no absorption for $\hbar\omega$. The imaginary part of conductance, $\sigma_2(\omega)$, can be calculated from $\sigma_1(\omega)$ by using Kramers-Kronig relations. The dielectric function $\varepsilon(\omega)$ can also be calculated from $\sigma(\omega)$ by using[26]

$$\varepsilon(\omega) = 1 + \frac{4\pi i}{\omega}\sigma(\omega). \tag{4}$$

In other words, starting from $\sigma_1(\omega)$, we can calculate pretty much all the optical properties of graphene nanoribbons, including the refraction index and reflectivity.

When calculating the matrix element $\langle n,k|P_x|n',k\rangle$ in Eq. (3), we only consider the effect of nearest neighbors, and we use $\langle i|\nabla|j\rangle = M\hat{\mathbf{e}}_{ij}$, where $M=0.206$ and $\hat{\mathbf{e}}_{ij}$ is the unit vector connecting from site i to site j.[24] It should be mentioned that the value of M does not affect the shape of $\sigma_1(\omega)$; therefore, the shape of the optical absorption spectrum is independent of the numerical value of M.

III. RESULTS AND DISCUSSION

First, we compare the optical response of (6, 6) SWNT and 12-ZGNR. As discussed in Sec. I, these two systems have similar atomic structure. However, the eigenstates $|n,k\rangle$ of ZGNR have different symmetric properties from the eigenstates of SWNT. In 12-ZGNR, due to the finite width and the potential being symmetric along the transverse direction (y direction), the eigenstates are either symmetric or antisymmetric along the y direction, namely, $\langle -y|n,k\rangle = \pm\langle y|n,k\rangle$. This symmetry property of ZGNR makes its selection rule for interband transitions qualitatively different from that of SWNT, as shall be discussed later.

In Fig. 1, the band structure of (6, 6) SWNT and 12-ZGNR is plotted in panels (a) and (b), respectively. In Fig. 1(a), we use different colors and formats to represent different subband indices for SWNT.[1,21,25] In Fig. 1(b), we use

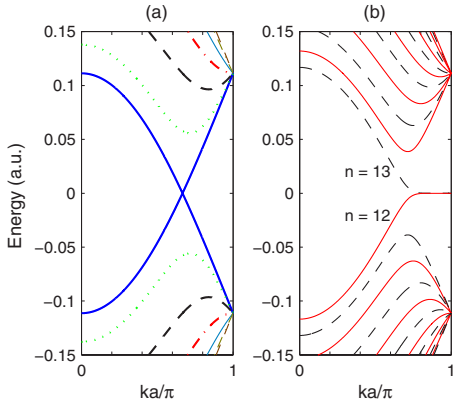

FIG. 1. (Color online) Band structure of (a) (6, 6) SWNT and (b) 12-ZGNR. For the case of (6, 6) SWNT, different colors and formats represent different subband indices (Refs. 1, 21, and 25). For the case of 12-ZGNR, black dashed lines (odd n) represent transversely symmetric states, and red solid lines (even n) represent transversely antisymmetric states. In both cases, only the transitions between the states with the same color and format are possible when the polarization of the incident beam is along the longitudinal direction.

black dashed lines to represent the transversely symmetric states and red solid lines to represent transversely antisymmetric states. For 12-ZGNR, an eigenstate $|n,k\rangle$ is symmetric if n is odd ($n=1$ being the state with lowest energy for a given k) and antisymmetric if n is even. When the incident beam is polarized longitudinal to SWNT, only the transitions between states with the same subband index are allowed. In the case of nanoribbons, only transitions between states with the same parity are allowed. In other words, only states with the same color and format in Fig. 1 can have interband transition. Next, we will use JDOS $D_j(\omega)$ and real conductance $\sigma_1(\omega)$ to demonstrate this selection rule.

In Figs. 2 and 3, JDOS $D_j(\omega)$ and real conductance $\sigma_1(\omega)$ are plotted. In each figure, panel (a) is for (6, 6) SWNT and panel (b) is for 12-ZGNR. Let us start by discussing the case of (6, 6) SWNT. In Fig. 2(a), we see peaks at different ω known as van Hove singularities. Consider the peaks at $\omega = 0.1114$, 0.1573, and 0.1929 a.u., for example. From Fig.

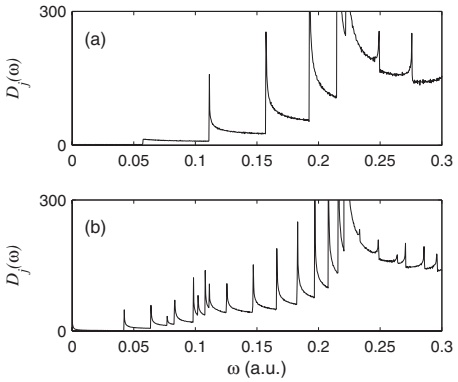

FIG. 2. Joint density of states $D_j(\omega)$ for (a) (6, 6) SWNT and (b) 12-ZGNR. Peaks in $D_j(\omega)$ are known as van Hove singularities. The effects of dipole matrix elements and selection rules are *not* considered here.

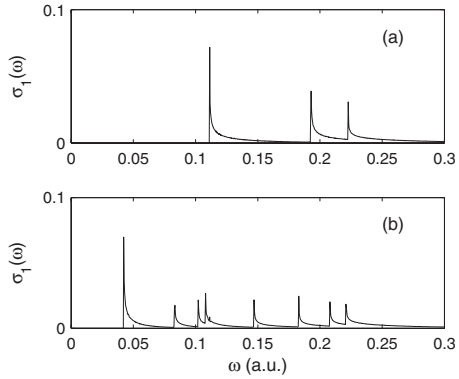

FIG. 3. Real part of the conductance $\sigma_1(\omega)$ for (a) (6, 6) SWNT and (b) 12-ZGNR. Peaks in $\sigma_1(\omega)$ indicate strong absorption for photons with energy $\hbar\omega$, and vanishing $\sigma_1(\omega)$ indicates no absorption. Notice how the peaks correspond to the allowed transition states shown in Fig. 1.

1(a), we see that the green subbands (thick dotted lines) at $k=0.715\pi/a$ and the black subbands (thick dashed lines) at $k=0.829\pi/a$ have vanishing derivatives, $\partial E/\partial k$, which cause the peaks of $D_j(\omega)$ in Fig. 2(a) to occur at $\omega=0.1114$ and 0.1929 a.u., respectively. At $k\approx 0.762\pi/a$ in Fig. 1(a), the green and black subbands below E_F have the same derivative with the black and green subbands above E_F, respectively. This is the reason that $D_j(\omega)$ in Fig. 2(a) has a peak at $\omega=0.1573$ a.u. However, the dipole matrix element $\langle$green, $0.762\pi/a|P_x|$ black, $0.762\pi/a\rangle$ vanishes; in other words, such a transition is forbidden. Therefore, as shown in Fig. 3(a), $\sigma_1(\omega)$ does not have a peak at $\omega=0.1573$ a.u., but it does have peaks at $\omega=0.1114$ and 0.1929 a.u. Another peak in Fig. 3(a) occurs at $\omega=0.2227$ a.u. This peak results from the transition between the red subbands (thick dot-dashed lines) in Fig. 1(a) at $k\approx\pi/a$. Notice that $\sigma_1(\omega)=0$ for $0<\omega<0.1114$ a.u., which appears to contradict the fact that (6, 6) SWNT is metallic and the blue subbands (thick solid lines) in Fig. 1(a) have energy gaps between 0 and 0.1114 a.u. The interband transition between the blue subbands does not occur because those states are also the eigenstates of momentum P_x.[21,25] Therefore, the off diagonal matrix elements in Eq. (3) are zero, and the transition cannot occur.

As discussed in the previous paragraph, the interband transitions of SWNT occur at the direct gaps at $k=0.715\pi/a$, $k=0.829\pi/a$, and $k\approx\pi/a$ for green, black, and red subbands, respectively. For GNR, however, direct-gap transitions cannot occur when the incident beam is polarized along the longitudinal direction. In Fig. 1(b), we see that the subband $E_{n,k}$ with $n=11$ (black dashed line) has a maximum at $k=0.714\pi/a$, and the subband with $n=14$ (red solid line) has a minimum at the same k. In other words, there is a direct gap between $n=11$ and 14 at $k=0.714\pi/a$. This direct gap makes $D_j(\omega)$, as shown in Fig. 2(b), peak at $\omega=0.0772$ a.u., which is the energy difference of these two states. However, the parity of these two states is different, and the transition is forbidden. Therefore, there is no peak at $\omega=0.0772$ a.u. in $\sigma_1(\omega)$, as shown in Fig. 3(b). We also see a peak at $\omega=0.0639$ a.u. in $D_j(\omega)$, which results from the energy gap at

TABLE I. Absorption peaks (shown in Fig. 3) that involve the transition from (to) the edge states $|n,k\rangle$ ($|n',k\rangle$), with $n=12$ ($n'=13$).

ω (a.u.)	k (π/a)	(n,n')	(n,n')
0.0423	0.741	(12, 14)	(11, 13)
0.0834	0.801	(12, 16)	(9, 13)
0.1081	0.929	(12, 18)	(7, 13)

$k=0.750\pi/a$ between $n=12$ and 15. Again, due to parity, there is no optical absorption at $\omega=0.0639$ a.u., as shown in Fig. 3(b). Although 12-ZGNR is metallic, its $\sigma_1(\omega)$ vanishes at low frequency, just like the case for (6, 6) SWNT. The reason is that for 12-ZGNR, states with $n=12$ and $n=13$ have different parity, which forbids the transition.

In ZGNRs, there exist edge states: The electronic states that are localized on the edge and decay exponentially into the center. For 12-ZGNR, the edge states are $|n,k\rangle$, with $n=12$ and 13 for $k>0.74$. The edge states play an important role in the interband transitions in optical range. In Fig. 3(b), the peaks at $\omega=0.0423$, 0.0834, and 0.1081 a.u. are due to edge states. The initial states $|n,k\rangle$ and final states $|n',k\rangle$ of these transitions are listed in Table I. The absorption peaks beyond $\omega=0.1081$ a.u. have nothing to do with the edge states, which can be seen from the band structure shown in Fig. 1(b). Note that both (6, 6) SWNT and 12-ZGNR have an absorption peak at $\omega\approx 0.221$ a.u., which results from the allowed transition at $k\approx\pi/a$, $E_{n,k}\approx\pm 0.111$ a.u.

We make a comparison of (10, 10) SWNT and 20-ZGNR in Figs. 4 and 5. The optical response is similar to the case for (6, 6) SWNT and 12-ZGNR because the selection rules do not change with the diameter of SWNT or the width of ZGNR. The only difference is that for the SWNT with

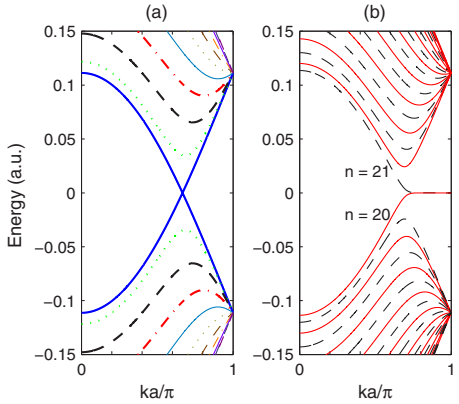

FIG. 4. (Color online) Band structure of (a) (10, 10) SWNT and (b) 20-ZGNR. For the case of (10, 10) SWNT, different colors and formats represent different subband indices (Refs. 1, 21, and 25). For the case of 20-ZGNR, black dashed lines (odd n) represent transversely symmetric states, and red solid lines (even n) represent transversely antisymmetric states. In both cases, only the transitions between the states with the same color and format are possible when the polarization of the incident beam is along the longitudinal direction.

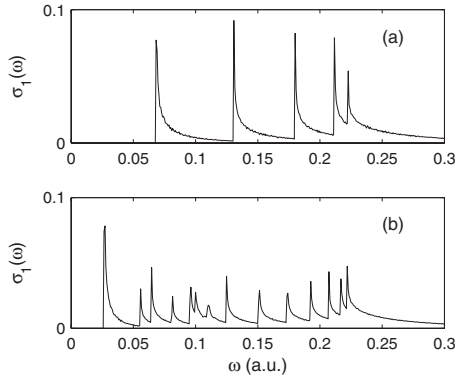

FIG. 5. Real part of the conductance $\sigma_1(\omega)$ for (a) (10, 10) SWNT and (b) 20-ZGNR. Peaks in $\sigma_1(\omega)$ indicate strong absorption for photons with energy $\hbar\omega$, and vanishing $\sigma_1(\omega)$ indicates no absorption. Notice how the peaks correspond to the allowed transition states shown in Fig. 4.

greater diameter and ZGNR with greater width, there are more absorption peaks, as can be seen by comparing Figs. 3 and 5. This is because they have a greater number of states per unit length, which allows more transitions, as can be seen by comparing the band structures shown in Figs. 1 and 4. Again, edge states are involved in many of the absorption peaks for ZGNR, including $\omega=0.0265$, 0.0559, 0.0816, 0.1000, and 0.1102 a.u. in Fig. 5(b). The peak at $\omega=0.1102$ a.u. is related to the interband transition from (to) the edge states $n=20$ $(n'=21)$ at $k \approx \pi/a$ shown in Fig. 4(b). Beyond $\omega=0.1102$ a.u., no absorption peak is related to the edge states. From the previous discussion for 12- and 20-ZGNR, we see that $\omega \approx 0.11$ a.u. is the threshold beyond which no absorption peak is contributed by edge states, and this threshold is barely dependent on the width of nanoribbons. Similar to Fig. 3, we can see absorption peaks at $\omega \approx 0.222$ a.u. for both (10, 10) SWNT and 20-ZGNR. Like (6, 6) SWNT and 12-ZGNR, this peak also corresponds to the transition that occurs at $k \approx \pi/a$, $E_{n,k} \approx \pm 0.111$ a.u.

IV. CONCLUSION

In this paper, we have studied the optical response of zigzag-edge graphene nanoribbons within the tight-binding approximation, and we have compared it to the case of armchair single-walled carbon nanotubes. Although these two materials have somewhat similar atomic structure, their electronic structure and the symmetry of eigenstates are quite different. For zigzag-edge nanoribbons, the eigenstates are either transversely symmetric or antisymmetric, which makes their optical response qualitatively different from that of SWNTs. In the presence of laser beams polarized longitudinal to nanotubes or nanoribbons, the interband transitions in nanotubes can occur at direct gaps, while the direct-gap transition in nanoribbons is forbidden.

We have also demonstrated that the edge states play an important role in the optical absorption of nanoribbons. They are involved in many of the absorption peaks in the optical range. The greatest photon energy with which edge states can cause an absorption peak is around 0.11 a.u., and we can always see an absorption peak around 0.11 a.u. for zigzag-edge nanoribbons with even number of zigzag lines. Beyond this threshold, which happens to be close to the boundary of optical range, edge states have no contribution to absorption peaks.

ACKNOWLEDGMENT

The authors would like to thank the Robert A. Welch Foundation (Grant No. F-1051) for their support.

[1] R. Saito, G. Dresselhaus, and M. S. Dresselhaus, *Physical Properties of Carbon Nanotubes* (Imperial College Press, London, 1998), and references therein.
[2] Steven G. Louie, Top. Appl. Phys. **80**, 113 (2001), and references therein.
[3] Kyoko Nakada, Mitsutaka Fujita, G. Dresselhaus, and M. S. Dresselhaus, Phys. Rev. B **54**, 17954 (1996).
[4] Yoshiyuki Miyamoto, Kyoko Nakada, and Mitsutaka Fujita, Phys. Rev. B **59**, 9858 (1999).
[5] Takazumi Kawai, Yoshiyuki Miyamoto, Osamu Sugino, and Yoshinori Koga, Phys. Rev. B **62**, R16349 (2000).
[6] Motohiko Ezawa, Phys. Rev. B **73**, 045432 (2006).
[7] Young-Woo Son, Marvin L. Cohen, and Steven G. Louie, Phys. Rev. Lett. **97**, 216803 (2006).
[8] L. Brey and H. A. Fertig, Phys. Rev. B **73**, 235411 (2006).
[9] Katsunori Wakabayashi, Mitsutaka Fujita, Hiroshi Ajiki, and Manfred Sigrist, Phys. Rev. B **59**, 8271 (1999).
[10] A. H. Castro Neto, F. Guinea, and N. M. R. Peres, Phys. Rev. B **73**, 205408 (2006).
[11] Dmitry A. Abanin, Patrick A. Lee, and Leonid S. Levitov, Phys. Rev. Lett. **96**, 176803 (2006).
[12] N. M. R. Peres, A. H. Castro Neto, and F. Guinea, Phys. Rev. B **73**, 195411 (2006).
[13] Denis A. Areshkin, Daniel Gunlycke, and Carter T. White, Nano Lett. **7**, 204 (2006).
[14] D. Gunlycke, H. M. Lawler, and C. T. White, Phys. Rev. B **75**, 085418 (2007).
[15] Young-Woo Son, Marvin L. Cohen, and Steven G. Louie, Nature (London) **444**, 347 (2006).
[16] C. L. Lu, C. P. Chang, Y. C. Huang, R. B. Chen, and M. L. Lin, Phys. Rev. B **73**, 144427 (2006).
[17] Takahiro Yamamoto, Tomoyuki Noguchi, and Kazuyuki Watanabe, Phys. Rev. B **74**, 121409(R) (2006).
[18] Hiroshi Ajiki and Tsuneya Ando, Physica B **201**, 349 (1994).
[19] M. F. Lin and Kenneth W.-K. Shung, Phys. Rev. B **50**, 17744 (1994).
[20] Shuichi Tasaki, Koji Maekawa, and Tokio Yamabe, Phys. Rev. B **57**, 9301 (1998).
[21] A. Gruneis, R. Saito, Ge. G. Samsonidze, T. Kimura, M. A. Pimenta, A. Jorio, A. G. Souza Filho, G. Dresselhaus, and M. S.

Dresselhaus, Phys. Rev. B **67**, 165402 (2003).
[22] M. Machon, S. Reich, C. Thomsen, D. Sanchez-Portal, and P. Ordejon, Phys. Rev. B **66**, 155410 (2003).
[23] G. Y. Guo, K. C. Chu, Ding-sheng Wang, and Chun-gang Duan, Phys. Rev. B **69**, 205416 (2004).
[24] Ashish Kumar Gupta, Ofir E. Alon, and Nimrod Moiseyev, Phys. Rev. B **68**, 205101 (2003).
[25] Han Hsu and L. E. Reichl, Phys. Rev. B **74**, 115406 (2006).
[26] Michael P. Marder, *Condensed Matter Physics* (Wiley, New York, 2000).